

# Bifurcation Diagrams of Population Models with Nonlinear Diffusion <sup>\*†‡</sup>

Young He Lee, Lena Sherbakov, Jackie Taber

Department of Mathematics, The College of William and Mary, Williamsburg, VA 23187, USA  
and

Junping Shi<sup>§</sup>

Department of Mathematics, College of William and Mary, Williamsburg, VA 23187, USA  
and, School of Mathematics, Harbin Normal University, Harbin, Heilongjiang, 150080, P.R.China

## Abstract

We develop analytical and numerical tools for the equilibrium solutions of a class of reaction-diffusion models with nonlinear diffusion rates. Such equations arise from population biology and material sciences. We obtain global bifurcation diagrams for various nonlinear diffusion functions and several growth rate functions.

## 1 Introduction

Diffusion mechanism models the movement of many individuals in an environment or media. The individuals can be very small such as basic particles in physics, bacteria, molecules, or cells, or very large objects such as animals, plants, or certain kind of events like epidemics, or rumors. By using the random walk or Fick's law, one can derive a one-dimensional reaction-diffusion model (see [9, 10, 21]):

$$(1.1) \quad \frac{\partial u}{\partial t} = \frac{\partial}{\partial x} \left( D \frac{\partial u}{\partial x} \right) + f(u),$$

where  $u(x, t)$  is the density function of the organism on a one-dimensional spatial domain, the diffusion rate  $D$  is a constant, and  $f(u)$  is the growth rate. However in some situations,

---

\*2000 subject classification: 35J65, 35B32

†Keywords: Global Bifurcation, Semilinear Elliptic Equation, Nonlinear Diffusion

‡This research is partially supported by NSF grant DMS-0314736. Junping Shi is also supported by College of William and Mary summer research grants, and a grant from Science Council of Heilongjiang Province, China.

§Corresponding author, email: shij@math.wm.edu

the random walk can be biased and the diffusion rate can depend on the density of the population. In [21, 20], Turchin derives a partial differential equation model with nonlinear diffusion:

$$(1.2) \quad \frac{\partial u}{\partial t} = \frac{\partial}{\partial x} \left( D(u) \frac{\partial u}{\partial x} \right) + f(u),$$

where  $D(u)$  is a positive cubic function; and another model of animal dispersal is also of form (1.2) with  $D(u) = u^m$  for some  $m > 0$  (see [9, 10].) Such model also appears as the porous media equation (with  $D(u) = u^m$  again) in material science (see [4].)

In this paper, we use analytic and numerical tools to consider the equilibrium solutions of (1.2) with Dirichlet boundary conditions  $u(0, t) = u(L, t) = 0$ . These conditions are appropriate for investigating species that are bound to their habitat (*i.e.*, if they leave outside of their boundary, they will die off immediately). After a nondimensionalization scaling, we consider the equation:

$$(1.3) \quad [D(u)u']' + \lambda f(u) = 0, \quad u(0) = u(1) = 0,$$

where  $D(u)$  is a nonnegative smooth function defined on  $\mathcal{R}^+$ , and  $\lambda$  is a positive parameter. Note that if  $D(u)$  is now a dimensionless diffusion function, then  $\lambda = L^2/D$ , where  $L$  is the length of the interval, and  $D$  is a scale of the diffusion rate. Thus a larger  $\lambda$  is equivalent to larger habitat size and slower diffusion.

For the nonlinear growth rate  $f(u)$ , we will consider three different growth patterns: (a) logistic growth; (b) weak Allee effect; and (c) strong Allee effect. In general, the logistic growth is characterized by a non-increasing growth rate per capita  $f(u)/u$ , and the Allee effect is when the growth rate per capita changes from increasing to decreasing as the population density increases. In the latter case, if the growth rate is positive at zero population, then it is called weak Allee effect, and if negative, then it is strong Allee effect. A more detailed discussion has been given in [15]. In this paper, for the sake of simplicity, we will only consider the representing examples of each case, (a) logistic  $f(u) = u(1 - u)$ ; (b) weak Allee effect  $f(u) = ku(1 - u)(u + b)$  for some  $k > 0$  and  $b \in (0, 1)$ ; and (c) strong Allee effect  $f(u) = ku(1 - u)(u - b)$  for some  $k > 0$  and  $b \in (0, 1)$ .

Following earlier works [19] for the case of  $D(u) \equiv 1$  (*i.e.* linear diffusion case), we develop analytic formulas for the bifurcation diagrams of positive solutions to (1.3). These formulas are generalizations of well-known time-mapping which is used to calculate the periods of nonlinear oscillators when  $D(u)$  is a constant function. The bifurcation diagrams of (1.3) when  $D(u) \equiv 1$  have been considered in [19, 8, 7, 12, 22, 6, 23], and Schaaf [12] also briefly considers the case of nonlinear  $D(u)$  but different situations. Cantrell and Cosner [1, 2, 3], Shi and Shivaji [17] study the equilibrium solutions of (1.3) in a more general setting, but their methods are quite different and our results here are more specific. An alternative approach to the bifurcation diagram is to use a transformation  $v = \int D(u)du$ , and to consider the equation  $v'' + \lambda f(u^{-1}(v)) = 0$  (see [17]), but practically the inverse of  $v$  is often difficult to calculate, and our approach here is more direct. The derivation

of the formulas are given in Section 2, and some analytic results on the monotonicity of the diagrams are also given in the same section. In Section 3, we discuss the numerical computation of the bifurcation diagrams with symbolic language `Maple`, and numerical computed diagrams for various scenarios are presented.

## 2 Generalized Time Mapping

By using a change of variable  $v = D(u)u'$ , we can convert the equation in (1.3) into a first order system:

$$(2.1) \quad u' = \frac{v}{D(u)}, \quad v' = -\lambda f(u).$$

A positive solution  $u$  of (1.3) corresponds to a solution  $(u, v)$  of (2.1) with  $u(0) = u(1) = 0$  and  $u(x) > 0$  for  $x \in (0, 1)$ . From the phase portraits of the system (2.1), such solution must be an orbit starting off from the positive  $v$ -axis, moving to the right until it reaches the positive  $u$ -axis, and returning to the negative  $v$ -axis. And the orbit is symmetric with respect to the  $u$ -axis. In particular, all the positive solutions  $u$  of (1.3) are symmetric with respect to  $x = 1/2$ ,  $u(x)$  is increasing in  $(0, 1/2)$ , and  $u(x)$  achieves the maximum value at  $x = 1/2$ .

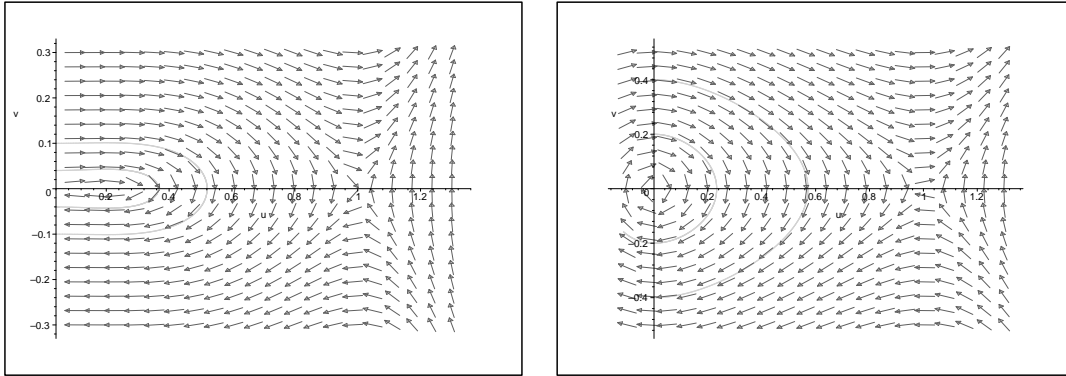


Figure 1: Phase portraits **(a)**  $D(u) = 1 - u + u^2$ ,  $f(u) = u(1 - u)$ ; **(b)**  $D(u) = u$ ,  $f(u) = u(1 - u)(u - 0.2)$

We multiply (2.1) by  $D(u)u'$ , and integrate it from  $t = 1/2$  to  $t = x > 1/2$ :

$$\int_{1/2}^x \frac{d}{dt} \left( \frac{[D(u)u']^2}{2} \right) dt + \lambda \int_{1/2}^x f(u)D(u)u' dt = 0.$$

Thus we obtain

$$\frac{[D(u(t))u'(t)]^2}{2} \Big|_{1/2}^x + \lambda \int_{u(1/2)}^{u(x)} f(u)D(u)du = 0,$$

From (2.2) and  $u'(1/2) = 0$ , we obtain

$$(2.2) \quad D(u) \frac{du}{dx} = -\sqrt{2\lambda[G(s) - G(u)]},$$

where  $s = u(1/2)$ ,  $u = u(x)$ , and  $G(u) = \int_0^u f(w)D(w)dw$ . Thus

$$(2.3) \quad \frac{dx}{du} = -\frac{1}{\sqrt{2\lambda}} \frac{D(u)}{\sqrt{G(s) - G(u)}}.$$

The sign in front of the square root is not  $\pm$  in this case because from  $u = 1/2$  to  $u = x$ , the slope of the curve is negative. Next we integrate (2.3) from  $u = u(1/2)$  to  $u = u(1) = 0$  (corresponding to  $x = 1/2$  to  $x = 1$ )

$$(2.4) \quad \frac{1}{2} = \int_{u(1/2)}^{u(1)} \frac{dx}{du} du = -\frac{1}{\sqrt{2\lambda}} \int_{u(1/2)}^{u(1)} \frac{D(u)}{\sqrt{G(s) - G(u)}} du.$$

So we obtain

$$(2.5) \quad \sqrt{\frac{\lambda}{2}} = \int_0^s \frac{D(u)}{\sqrt{G(s) - G(u)}} du \equiv T(s),$$

where  $s = u(1/2)$ , and

$$(2.6) \quad \lambda(s) = 2 \left( \int_0^s \frac{D(u)}{\sqrt{G(s) - G(u)}} du \right)^2 = 2[T(s)]^2.$$

Here  $\lambda(s)$  is a function well defined as long as  $G(s) - G(u) > 0$  for all  $u \in (0, s)$  and the integral  $T(s)$  is convergent. The convergence of the integral can be established if  $f(u)D(u)$  and  $D(u)$  are continuous in  $[0, s]$  and  $f(s)D(s) > 0$ . Indeed in this case  $G(u)$  is continuously differentiable, then we can conclude that  $T(s)$  is convergent via a comparison with the integral  $K \int_{s-\delta}^s (s-u)^{-1/2} du$  where  $K$  is associated with the bounds of  $D(u)$  and  $f(s)D(s)$ . Since we assume that  $D(s) > 0$  for all  $s > 0$ , then the domain of the generalized time-mapping function  $T(s)$  is

$$(2.7) \quad \mathcal{D} = \{s > 0 : f(s) > 0, \int_u^s f(t)D(t)dt > 0 \text{ for all } u \in [0, s]\}.$$

We notice that  $f(0) = 0$ , then  $u = 0$  is always a solution of (1.3) for any  $\lambda > 0$ . Often a branch of non-zero solutions bifurcates from the line of the trivial solutions  $\{(\lambda, 0)\}$ . In that case  $\mathcal{D}$  includes an interval  $(0, \delta)$  for some  $\delta > 0$ , and the bifurcation point  $\lambda_*$  on the line of trivial solutions can be calculated through a limit of the time-mapping.

**Proposition 2.1.** *Suppose that  $f(u) \geq 0$  for  $u \in [0, \delta]$  for some  $\delta > 0$ .*

1. If  $f(0) = 0$  and  $f'(0) > 0$ , then

$$(2.8) \quad \lim_{s \rightarrow 0^+} T(s) = \frac{\pi \sqrt{D(0)}}{\sqrt{2f'(0)}},$$

and the bifurcation point is  $\lambda_* = D(0)\pi^2/f'(0)$ ;

2. If  $f(0) = 0$  and  $f'(0) = 0$ , then  $\lim_{s \rightarrow 0^+} T(s) = \lim_{s \rightarrow 0^+} \lambda(s) = \infty$ ;

3. If  $f \in C^1(\mathcal{R}) \cap C^0(\overline{\mathcal{R}})$ ,  $f(0) = 0$ , and  $\lim_{s \rightarrow 0^+} f'(u) = \infty$ , then  $\lim_{s \rightarrow 0^+} T(s) = \lim_{s \rightarrow 0^+} \lambda(s) = 0$ ;

4. If  $f(0) > 0$ , then  $\lim_{s \rightarrow 0^+} T(s) = \lim_{s \rightarrow 0^+} \lambda(s) = 0$ .

*Proof.* We derive the formula following a calculation in [14], and alternative proofs can also be found in [12] and [6]. In the proof we will use the following simple fact: suppose that

$$(2.9) \quad (a - \eta)u \leq g(u) \leq (a + \eta)u, \quad \text{for } u \in [0, \delta],$$

where  $a, \delta > 0$ ,  $0 < \eta < a/2$ . Then for  $G(u) = \int_0^u g(t)dt$ ,

$$(2.10) \quad \frac{a - \eta}{2}(u^2 - v^2) \leq G(u) - G(v) \leq \frac{a + \eta}{2}(u^2 - v^2),$$

for any  $0 \leq v < u \leq \delta$ . The proof of (2.10) can be done by considering  $\Gamma(u) = G(u) - G(v) - (1/2)(a + \eta)(u^2 - v^2)$ . We observe that  $\Gamma(v) = 0$ ,  $\Gamma'(u) = g(u) - (a + \eta)u \leq 0$  for  $u \in [v, \delta]$  by (2.9), then  $\Gamma(u) \leq 0$  for  $u \in [v, \delta]$ . The proof for the other part is similar.

First we assume  $f(0) = 0$ ,  $f'(0) > 0$  and  $D(0) > 0$ . Let  $g(u) = f(u)D(u)$ . Then  $g(0) = 0$  and for any  $\eta > 0$  and  $\eta < f'(0)D(0)/2$ , there exists  $\delta > 0$  such that

$$(2.11) \quad [g'(0) - \eta]u \leq g(u) \leq [g'(0) + \eta]u, \quad \text{for } u \in [0, \delta].$$

By further restricting  $\delta$ , we can also assume that

$$(2.12) \quad D(0) - \eta u \leq D(u) \leq D(0) + \eta u, \quad \text{for } u \in [0, \delta].$$

By using (2.10), (2.11) and (2.12), we obtain

$$(2.13) \quad \begin{aligned} T(s) &= \int_0^s \frac{D(u)}{\sqrt{G(s) - G(u)}} du \leq \int_0^s \frac{\sqrt{2}(D(0) + \eta)u}{\sqrt{(g'(0) - \eta)(s^2 - u^2)}} du \\ &= \frac{\sqrt{2}D(0)}{\sqrt{(g'(0) - \eta)}} \int_0^s \frac{du}{\sqrt{s^2 - u^2}} + \frac{\sqrt{2}\eta}{\sqrt{(g'(0) - \eta)}} \int_0^s \frac{udu}{\sqrt{s^2 - u^2}} \\ &= \frac{D(0)\pi}{\sqrt{2(g'(0) - \eta)}} + \frac{2\sqrt{2}\eta s}{\sqrt{(g'(0) - \eta)}}, \end{aligned}$$

for any  $s \in [0, \delta]$ . Similarly we can show that

$$(2.14) \quad T(s) \geq \frac{D(0)\pi}{\sqrt{2(g'(0) + \eta)}} - \frac{2\sqrt{2}\eta s}{\sqrt{(g'(0) + \eta)}}$$

for any  $s \in [0, \delta]$ . Since  $\eta$  can be chosen arbitrarily, and  $g'(0) = f'(0)D(0)$ , then we obtain (2.8). The other cases can all be proved along the similar line.  $\square$

For further calculation of the time-mapping, we often use the following change of variables:

$$(2.15) \quad T(s) = \int_0^s \frac{D(u)}{\sqrt{2(G(s) - G(u))}} du = \int_0^1 \frac{sD(sw)}{\sqrt{G(s) - G(sw)}} dw$$

By differentiation, we obtain

$$\begin{aligned} T'(s) &= \int_0^s \frac{2[D(sw) + swD'(sw)][G(s) - G(sw)] - sD(sw)[G'(s) - wG'(sw)]}{2[G(s) - G(sw)]^{3/2}} dw \\ &= \int_0^s \frac{D(sw)[2G(s) - sG'(s) - 2G(sw) - swG'(sw)] + 2swD'(sw)[G(s) - G(sw)]}{2[G(s) - G(sw)]^{3/2}} dw \\ &= \int_0^s \frac{D(sw)[H_g(s) - H_g(sw)] + 2swD'(sw)[G(s) - G(sw)]}{2[G(s) - G(sw)]^{3/2}} dw \end{aligned}$$

where  $H_g(u) = 2G(u) - uG'(u)$ . From this representation of  $T'(s)$ , we can easily obtain the following result regarding the monotonicity of the bifurcation diagram:

**Proposition 2.2.** *Suppose that  $s \in \mathcal{D}$ .*

1. *If  $H_g(s) > H_g(u)$  for any  $u \in (0, s)$ , and  $D'(s) \geq 0$  for any  $s > 0$ , then  $T'(s) \geq 0$ ;*
2. *If  $2D(u) + uD'(u) > 0$  and  $sf(s)D(s) < uf(u)D(u)$  for any  $u \in (0, s)$ , then  $T'(s) \geq 0$ .*

Although the proof of Proposition 2.2 is obvious, the conditions in the proposition are usually not easy to check, or are not satisfied for the practical problems we consider. But it does cover the well-known case of logistic equation with linear diffusion:

**Corollary 2.3.** *Suppose that the growth rate function is the logistic type such that  $f(0) = f(M) = 0$  and  $f(u) > 0$  in  $(0, M)$  for some  $M > 0$ ,  $[f(u)/u]' \leq 0$  for  $u \in (0, M)$ , and  $D(u) \equiv k > 0$ . Then the bifurcation diagram of (1.3) is monotone increasing.*

*Proof.* We can verify that  $H'_g(s) \geq 0$  in  $(0, M)$  since  $[f(u)/u]' \leq 0$  for  $u \in (0, M)$ . thus  $T'(s) > 0$  for  $s \in (0, M)$ .  $\square$

For the power function diffusion rate and the quadratic logistic type, a similar result can be obtained:

**Proposition 2.4.** *Suppose that the growth rate function is the logistic type  $f(u) = u(1 - u)$ , and the diffusion function  $D(u) = u^m$  for  $m > 0$ . Then the bifurcation diagram of (1.3) is monotone increasing.*

*Proof.* From calculations with `Maple`, we have

$$D(sw)[H_g(s) - H_g(sw)] + swD'(sw)[G(s) - G(sw)] = \frac{(w^m - w^{3+2m})s^{3+2m}}{m + 3} > 0,$$

for any  $w \in (0, 1)$ . □

Detailed analytical and qualitative approach to the time-mapping when  $D(u) = 1$  has been extensively carried out in, for example, [19, 6, 16, 22, 23]. In a forthcoming paper [18], analytic results on bifurcation diagrams with turning points will be studied.

### 3 Numerical Results

In this section, we present numerical bifurcation diagrams of (1.3) for various diffusion function  $D(u)$  and growth rate function  $f(u)$ . The numerical bifurcation diagrams are calculated with symbolic mathematical software `Maple` (Version 8). To calculate the time-mapping  $T(s)$ , we first find the domain  $\mathcal{D}$  of the function  $T(s)$ , and in all cases we consider,  $\mathcal{D} = (a, b)$  for some  $b > a \geq 0$ . Next we discretize  $(a, b)$ :  $a = s_0 < s_1 < s_2 < \dots < s_N = b$ , where  $s_i = a + i\Delta s$  where  $\Delta s = (b - a)/N$ . For each  $s_i$ , we calculate  $T(s_i)$  by using the integral defined in (2.5), and the integral is computed numerically with the build-in integrator in `Maple`. Then the bifurcation diagram is generated by the set  $\{(\lambda(s_i), s_i) : 0 \leq i \leq N\}$ . In all the bifurcation diagrams this section,  $\lambda$  is the horizontal axis and  $d = u(\lambda, 0)$  is the vertical axis.

In the numerical studies, we consider the following cases:

1.  $D(u) = 1$ ,  $D(u) = u^m$  ( $m = 1, 2$ ), or  $D(u) = 1 - au + bu^2$  ( $a > 0, b > a^2/4$ ); and
2.  $f(u) = u(1 - u)$ ,  $f(u) = k_1u(1 - u)(u + b)$  ( $0 < b < 1$ ), or  $f(u) = k_2u(1 - u)(u - b)$  ( $0 < b < 1$ ).

#### Case 1: Logistic growth $f(u) = u(1 - u)$

The bifurcation diagram of linear diffusive logistic equation is well-known (see Figure 2 (a), also [3, 17].) When  $\lambda < \lambda_* = \pi^2$ , there is only the trivial solution  $u = 0$ ; and when  $\lambda > \lambda_*$ , there is a unique positive equilibrium solution  $u(\lambda, \cdot)$  of (1.3), and Figure 2 (a) gives the relation of  $\lambda$  and  $s = u(\lambda, 0)$ .

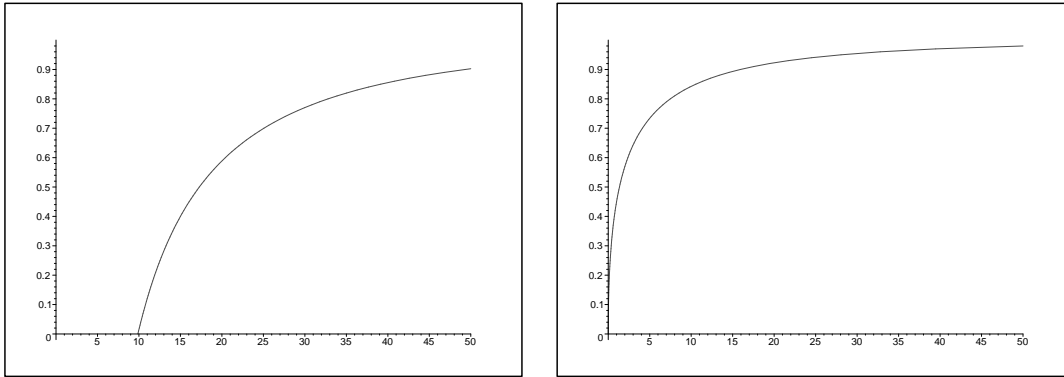


Figure 2: **(a)**  $D(u) = 1, f(u) = u(1 - u)$ ; **(b)**  $D(u) = u^2, f(u) = u(1 - u)$

We have shown in Proposition 2.4 that when  $D(u) = u^m$  ( $m > 0$ ), the bifurcation diagram is monotone increasing. Figure 2 (b) shows the diagram when  $D(u) = u^2$  and  $f(u) = u(1 - u)$ . In this case, there is a unique positive equilibrium solution  $u(\lambda, \cdot)$  of (1.3) for any  $\lambda > 0$ , and the bifurcation point is  $\lambda_* = 0$ . Moreover, the bifurcation diagram is tangent to the  $s$ -axis, which can be proved by calculating the time-mapping near  $s = 0$ .

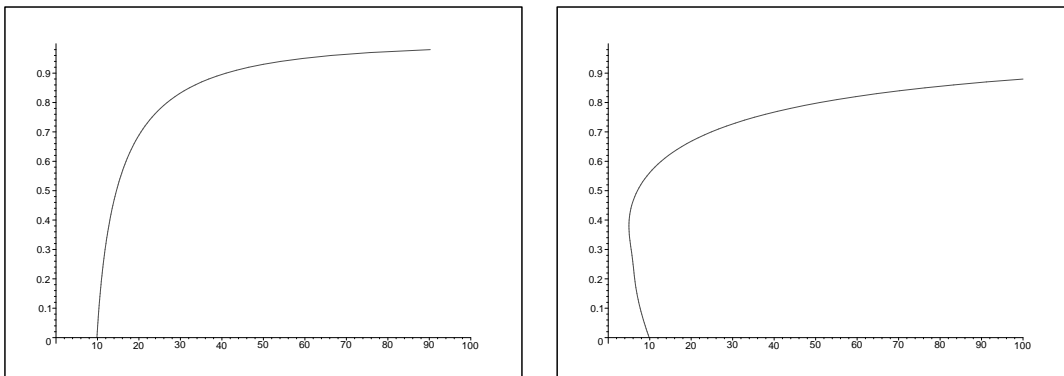


Figure 3: **(a)**  $D(u) = u^2 - u + 1, f(u) = u(1 - u)$ ; **(b)**  $D(u) = 17u^2 - 8u + 1, f(u) = u(1 - u)$

The case of quadratic  $D(u)$  has been studied in [1, 2, 17]. It is known that a subcritical bifurcation at  $\lambda = \lambda_*$  can occur if  $D'(0)$  is sufficiently negative, thus there exists  $\lambda^* \in (0, \lambda_*)$  such that (1.3) has at least two positive solutions when  $\lambda \in (\lambda^*, \lambda_*)$ . But when  $D'(0)$  is positive or  $D'(0)$  is not negative enough, then the bifurcation diagram is similar to that of constant diffusion case. Our numerical results verify these previous studies: Figure 3 (a) is the diagram when  $D'(0) = -1$ , and it is monotone; and Figure 3 (b) is the diagram when  $D'(0) = -8$ , and the bifurcation at  $\lambda = \lambda_*$  is subcritical. In both cases,  $\lambda_* = \pi^2$  since we keep  $D(0) = 1$ , and in the latter case, the turning point of the diagram  $\lambda^* \approx 5.00$  and the



corresponding  $s^* \approx 0.38$ . From a calculation similar to that in [13], we can find that

$$(3.1) \quad \lambda'(0) = \frac{4\pi}{3}[D'(0) + 2],$$

when  $f(u) = u(1 - u)$  and  $D(u)$  is differentiable at  $u = 0$ . Thus the bifurcation becomes subcritical if  $D'(0) < -2$ .

**Case 2: Weak Allee Effect Growth,  $f(u) = u(1 - u)(u + b)$  ( $0 < b < 1$ )**

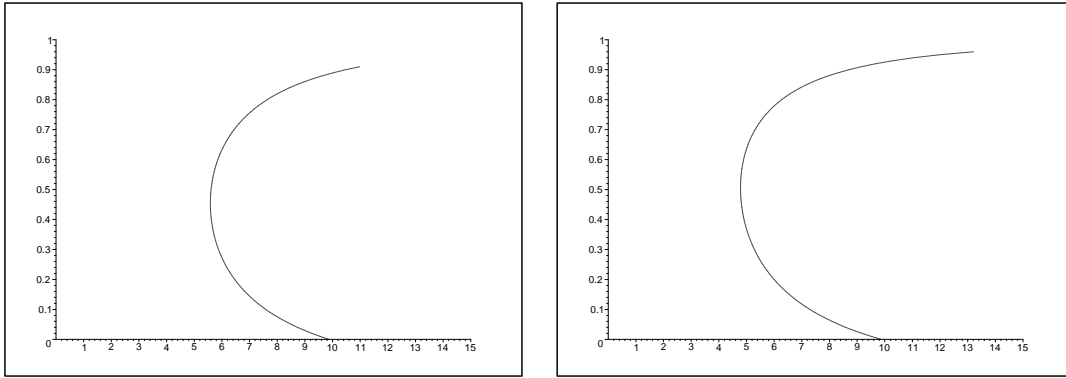


Figure 4: **(a)**  $D(u) = 1, f(u) = 5u(1 - u)(u + 0.2)$ ; **(b)**  $D(u) = u^2 - u + 1, f(u) = 5u(1 - u)(u + 0.2)$

If the growth rate is of weak Allee effect, then the bifurcation at  $\lambda = \lambda_*$  is subcritical even the diffusion function  $D(u)$  is constant (see proof in [17] and Figure 4 (a).) Thus the weak Allee effect causes conditional persistence of the population when the diffusion rate is not so large. Here conditional persistence means that the population will persist if the initial population is above certain threshold, and it will not if the initial population is below the threshold (see more detail discussions in the Introduction of [17].) Note that such conditional persistence can also be caused by nonlinear diffusion as in Figure 3 (b) and logistic growth rate, which was first discovered in [1]. When the diffusion function is quadratic, then the conditional persistence is enhanced by the slower diffusion when the population density  $u$  is between 0 and 1 (see Figure 4 (b).) In Figure 4 (a), the turning point is at  $(\lambda, s) = (5.582, 0.46)$ , while in Figure 4 (b), it is  $(\lambda, s) = (4.784, 0.51)$ . Notice that  $D(u) = 1 - u + u^2$  achieves the maximal diffusion rate at  $u = 0$  and  $u = 1$ , and  $D(u) < 1$  in  $(0, 1)$ . Thus smaller diffusion rate for mid-range density increases the critical  $\lambda^*$ , which implies the increasing of the critical patch size. In Figure 5 (a), the bifurcation point is at  $\lambda_* = 0$  since  $D(0) = 0$ , and in this case, the bifurcation diagram appears to be monotonely increasing with respect to  $\lambda$ .

**Case 3: Strong Allee Effect Growth,  $f(u) = u(1 - u)(u - b)$  ( $0 < b < 1$ )**

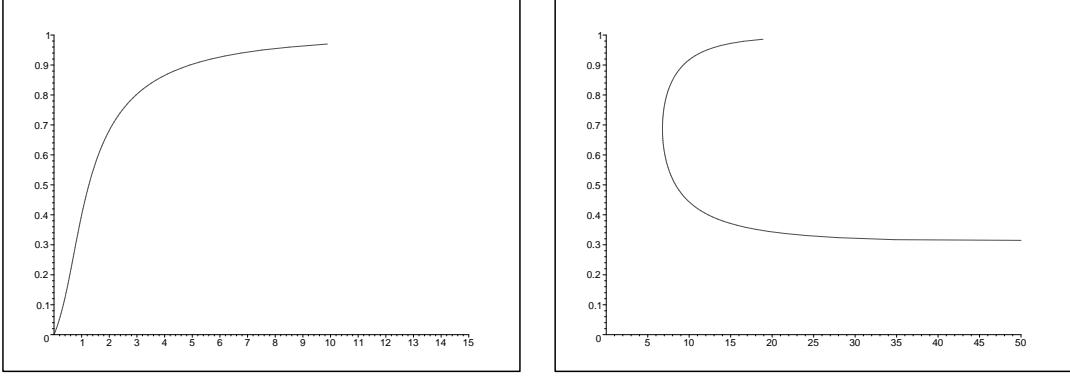


Figure 5: **(a)**  $D(u) = u, f(u) = 5u(1-u)(u+0.2)$ ; **(b)**  $D(u) = 1, f(u) = 10u(1-u)(u-0.2)$

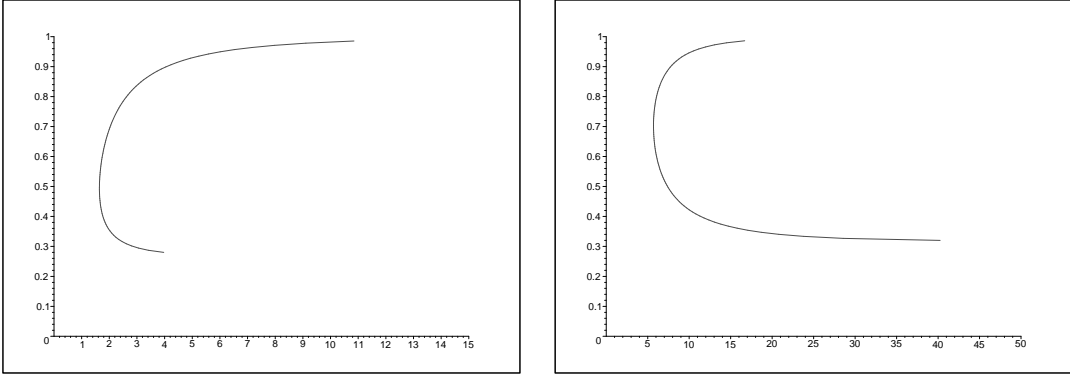


Figure 6: **(a)**  $D(u) = u, f(u) = 10u(1-u)(u-0.2)$ ; **(b)**  $D(u) = u^2 - u + 1, f(u) = 10u(1-u)(u-0.2)$

When  $D(u) = 1$ , the bifurcation diagram of (1.3) was first considered in [19], and the corresponding high dimensional version was also obtained in [11]. In this case, no bifurcation occurs along the line of  $u = 0$  since all small initial population will become extinct. There exists  $\lambda^* > 0$  such that (1.3) has no solution when  $\lambda < \lambda^*$ , and it has exactly two solutions when  $\lambda > \lambda^*$  (see Figure 5 (b), and the analytical exact multiplicity results was proved in [19, 11].) For strong Allee effect growth, the nonlinear diffusion has less impact on the structure of the bifurcation diagrams. When  $D(u)$  is a power function or a quadratic function, the bifurcation diagram is similar to that of linear diffusion (see Figure 5 (a,b).) The turning point on the diagram are: for  $D(u) = 1$ ,  $(\lambda^*, s^*) = (6.778, 0.685)$ ; for  $D(u) = u$ ,  $(\lambda^*, s^*) = (1.642, 0.492)$ ; and for  $D(u) = u^2 - u + 1$ ,  $(\lambda^*, s^*) = (5.697, 0.703)$ . In this set of diagrams, we choose  $f(u) = 10u(1-u)(u-0.2)$  so  $\max f(u)$  is comparable with that in weak Allee effect case. We also mention that the bifurcation diagram is indeed a  $\subset$ -shaped. And there are two horizontal asymptotes: the upper at  $s = 1$  (the zero of  $f(u)$ ) and the

lower at the unique zero of  $G(u) = \int_0^u D(t)f(t)dt$ . The numerical graphs above sometimes do not show the parts which tend to  $\lambda = \infty$  due to limitation of the algorithm, since the curve tend to the asymptote very fast. Comparing the diagram of  $D(u) = u$  (Figure 6 (a)) with the ones with  $D(u) > 0$  for all  $u$  (Figure 5 (b) and Figure 6 (b)), we can see that the diagram of  $D(u) = u$  leans toward the origin due to the degeneracy of the diffusion function. We also notice that the all these bifurcation diagrams can only be obtained when  $G(u) > 0$  for some positive  $u$ , otherwise (1.3) has only the zero solution.

## 4 Concluding Remarks

Analytical and numerical tools are employed to obtain the bifurcation diagrams of equilibrium solutions of reaction-diffusion models with nonlinear diffusion. The bifurcation points from the trivial solutions are identified and calculated, and for models with unique non-constant equilibrium, the bifurcation point is equivalent to the critical length of the habitat. The critical length is smaller than the one given by the bifurcation point when an Allee effect presents in the system. The Allee effect can be caused by non-monotonic intrinsic growth rate of the biological species as in Cases 2 or 3 above, but it can also happen as a result of nonlinear diffusion and monotone intrinsic growth rate as in Case 1.

## References

- [1] Cantrell, Robert Stephen; Cosner, Chris, Diffusive logistic equations with indefinite weights: population models in disrupted environments. II. *SIAM J. Math. Anal.* **22** (1991), no. 4, 1043–1064.
- [2] Cantrell, Robert Stephen; Cosner, Chris, Conditional persistence in logistic models via nonlinear diffusion. *Proc. Roy. Soc. Edinburgh Sect. A* **132** (2002), no. 2, 267–281.
- [3] Cantrell, Robert Stephen; Cosner, Chris, Spatial ecology via reaction-diffusion equation. *Wiley series in mathematical and computational biology*, John Wiley & Sons Ltd, 2003.
- [4] Diaz, J. I., Nonlinear partial differential equations and free boundaries. Vol. I. Elliptic equations. *Research Notes in Mathematics*, **106**. Pitman (Advanced Publishing Program), Boston, MA, 1985.
- [5] Kot, Mark, Elements of mathematical ecology. Cambridge University Press, Cambridge, 2001.
- [6] Logan, Roger, Positive solutions to a system of differential equations modeling a competitive interacting system with nonlogistic growth rates, *Differential and Integral equations*, **10**, (1997), no.5, 929–945.
- [7] Manoranjan, V. S. Bifurcation studies in reaction-diffusion. II. *J. Comput. Appl. Math.* **11** (1984), no. 3, 307–314.
- [8] Manoranjan, V. S.; Mitchell, A. R.; Sleeman, B. D.; Yu, Kuo Pen, Bifurcation studies in reaction-diffusion. *J. Comput. Appl. Math.* **11** (1984), no. 1, 27–37.

- [9] Murray, J. D., Mathematical biology. Third edition. I. An introduction. *Interdisciplinary Applied Mathematics*, **17**. Springer-Verlag, New York, 2002.
- [10] Okubo, Akira; Levin, Simon, Diffusion and ecological problems: modern perspectives. Second edition. *Interdisciplinary Applied Mathematics*, **14**. Springer-Verlag, New York, 2001.
- [11] Ouyang, Tiancheng; Shi, Junping, Exact multiplicity of positive solutions for a class of semilinear problem. *J. Differential Equations* **146** (1998), no. 1, 121–156.
- [12] Schaaf, Renate, Global solution branches of two-point boundary value problems. *Lecture Notes in Mathematics*, **1458**. Springer-Verlag, Berlin, 1990.
- [13] Shi, Junping, Persistence and bifurcation of degenerate solutions, *Jour. Func. Anal.* **169**, (1999), no. 2, 494–531.
- [14] Shi, Junping, Blow-up Points of Solution Curves for a Semilinear Problem. *Topo. Meth. of Nonlinear Anal.*, **15**, (2000), No. 2, 251–266.
- [15] Shi, Junping, Nonlinear reaction-diffusion equations, *Lecture Note*, (2004).
- [16] Shi, Junping; Shivaji, Ratnasinham, Exact Multiplicity of Solutions For Classes of Semipositone Problems With Concave-Convex Nonlinearity, *Discrete And Continuous Dynamical Systems*, **7**, (2001), no. 3, 559–571.
- [17] Shi, Junping; Shivaji, Ratnasinham, Persistence in Reaction Diffusion Models with Weak Allee Effect. Preprint, (2004).
- [18] Shi Junping; Taber, Jacky, in preparation.
- [19] Smoller Joel; Wasserman, Arthur, Global bifurcation of steady-state solutions, *J. Differential Equations*, **39**, (1981), no. 2, 269-290.
- [20] Turchin, Peter, Population consequences of aggregative movement. *Journal of Animal Ecology* **58** (1989), 75–100.
- [21] Turchin, Peter, Quantitative Analysis of Movement: Measuring and Modeling Population Redistribution in Animals and Plants. Sinauer Associates, Inc, 1998.
- [22] Wang, Shin-Hwa, On the time map of a nonlinear two point boundary value problem. *Differential and Integral Equations*, **7**, (1994) no. 1, 49-55.
- [23] Wang, Shin-Hwa; Yeh, Tzung-Shin, A complete classification of bifurcation diagrams of a Dirichlet problem with concave-convex nonlinearities. *J. Math. Anal. Appl.* **291** (2004), no. 1, 128–153.